JOURNAL OF CATALYSIS **171,** 231–244 (1997)
ARTICLE NO. CA971804

# The Making and Characterization of BaO- and $BaCl_2$-Promoted $Y_2O_3$ Catalysts for the OCM Reaction

C. T. Au,[1] Y. W. Liu, and C. F. Ng

*Department of Chemistry and Centre for Surface Analysis and Research, Hong Kong Baptist University, Kowloon Tong, Hong Kong*

Received March 4, 1997; revised June 26, 1997; accepted June 30, 1997

**The performances of the 30 mol% $MO/Y_2O_3$ ($M = Mg$, Ca, Sr, Ba) catalysts in OCM reactions have been investigated. The BaO-promoted one has out-performed the others. We found that the 30 mol% $BaX_2/Y_2O_3$ ($X = F$, Cl, Br) catalysts could do even better. Both $BaF_2$ and $BaCl_2$ are good materials to promote $Y_2O_3$. At 800°C and with $CH_4 : O_2 : N_2 = 2.47 : 1 : 11.4$, total flow rate = 50 ml $min^{-1}$, contact time = 0.6 g s $ml^{-1}$, and weight of catalyst = 0.5 g, the $C_2$ yields over the catalysts were respectively 19.7 and 22.3%. In this paper, we concentrate on the $BaCl_2/Y_2O_3$ catalysts and compare them with the $BaO/Y_2O_3$ ones. It is obvious that the 30 mol% $BaCl_2/Y_2O_3$ catalyst is superior to the 30 mol% $BaO/Y_2O_3$ one both in $C_2$ selectivity and $C_2H_4/C_2H_6$ ratio. XRD examinations revealed that the addition of 10–50 mol% of BaO or $BaCl_2$ has greatly altered the surface and bulk natures of $Y_2O_3$. Crystal phase of orthorhombic $BaCO_3$ was found to exist in the 30 mol% $BaO/Y_2O_3$ catalyst. Although no significant amount of any barium compound was detected over the fresh 30 mol% $BaCl_2/Y_2O_3$ catalyst, crystal phases of orthorhombic $Ba_3Cl_4CO_3$ and $BaCO_3$ were detected after OCM reactions. Also, the cubic $Y_2O_3$ lattices of the BaO- and $BaCl_2$-promoted catalysts were found to have undergone expansion which is a result of ionic substitution(s). The reactivity of the 30 mol% $BaCl_2/Y_2O_3$ catalyst has been monitored for 40 h at 750°C and found to be stable. Although XPS results suggested no significant change in surface chlorine concentration, analysis of Cl content of the catalyst revealed that up to ca 15.5% of the original content of chlorine was lost after 20 h of reaction. $Y_2O_3$ by itself lacks active oxygen for the oxidation reaction. $O_2$ TPD and reduction studies of the fresh 30 mol% BaO- and $BaCl_2$-promoted catalysts showed that the amount of active oxygen in the former was at least 4 times that in the latter. However, during OCM reaction, the 30 mol% $BaCl_2/Y_2O_3$ catalyst was changing somewhat like a 30 mol% $BaO/Y_2O_3$ catalyst. It is apparent that the presence of $Cl^-$ ions in the 30 mol% $BaCl_2/Y_2O_3$ catalyst is the reason for the superiority in $C_2$ selectivity over the $BaCl_2$-promoted $Y_2O_3$ catalysts. We conclude that the presence of $Ba^{2+}$ ions can enhance the amount of oxidative oxygen for $CH_4$ activation while the presence of $Cl^-$ suppresses deep oxidation. A careful balance of the two can optimize the performance of the Y–Ba–Cl catalysts in the OCM reaction.**

## INTRODUCTION

The utilization of natural gas, especially through the conversion of methane to useful chemicals such as ethene and methanol, has been widely studied. As far as the oxidative coupling of methane (OCM) reaction is concerned, a large number of compounds have been tried as catalysts. Among the materials studied, alkaline earth oxides or carbonates and rare earth oxides have been found to be active (1–8). Clear trends of augmentation in catalytic performance have been observed with the increase in basicity of the alkaline earth oxides: MgO < CaO < SrO < BaO (1, 7, 9, 10). It is obvious that the strongly basic SrO and BaO can give better $C_2$ selectivities (3, 5, 7). Korf *et al.* have showed a synergistic effect between Ca and Ba oxides. They suggested that the active oxygen species in the case of Ba/CaO is an $O_2^{2-}$ species (5). The use of rare earth oxides as catalysts has been studied extensively (7, 11–18). At 700°C and with contact time = 0.002 g s $ml^{-1}$ and $CH_4 : O_2 = 45.5 : 1$, the performance over the rare earth oxides was found to increase in the order of $CeO_2$, $TbO_x$, $PrO_x < Lu_2O_3$, $Dy_2O_3$, $Eu_2O_3$, $Nd_2O_3$, $La_2O_3$, $Y_2O_3$, $Yb_2O_3$, $Tm_2O_3 < Er_2O_3$, $Gd_2O_3 < Ho_2O_3 < Sm_2O_3$ (11a). Results of later research also suggested that rare earth oxides such as $Sm_2O_3$ (7, 11e), $Eu_2O_3$ (7), $Ho_2O_3$ (7), $Gd_2O_3$ (18), $La_2O_3$ (7, 15–18), and $Y_2O_3$ (17) are good materials for producing good-performance OCM catalysts.

Composite metal oxides containing rare earth have been thought to be good catalysts for the OCM reaction. Alkaline earth oxides have been found to be good promoting materials for rare earth oxides (17, 18, 20–25). For example, Deboy *et al.* found that while there was little change in $CH_4$ conversion (ca 20%), the $C_2$ selectivities over 1% $Sr/La_2O_3$ and 1% $Ba/La_2O_3$ were 65.4 and 68.1%, respectively, significantly higher than the value of 59.0% over $La_2O_3$ (21). Other composite catalysts such as $Ca/ThO_2$, $Sr/ThO_2$, $Ba/ThO_2$ (20) and $CaY_2$, $SrY_2$, $BaY_2$, $SrTh_2$, $SrLa_2$ (17) have been reported to be active for the OCM reaction. Osada *et al.* (26) have studied the binary oxides of $Y_2O_3$–CaO for the OCM reaction. They found that $C_{2+}$ selectivity at 700°C was affected by a lattice distortion of $Y_2O_3$ and increased

---

[1] To whom correspondence should be addressed. E-mail: pctau@hkbu.edu.hk.

0021-9517/97 $25.00

with the increasing content of $Y_2O_3$ in the coprecipitated catalyst. Kaminsky *et al.* (27) have studied the Ba-doped yttria oxidative coupling catalyst and proposed that the active site were charge-deficient oxygen sites created as $Ba^{2+}$ substitutes into $Y^{3+}$ lattice sites. More recently, the dissolution of $Sr^{2+}$ into $Y_2O_3$ has been suggested by Erarslanoglu *et al.* to be the reason for the higher performance of the $Sr/Y_2O_3$ (1 : 10 molar ratio) catalyst as compared to the undoped $Y_2O_3$ (28).

The effects of halides on the catalytic performance of MgO and CaO have been demonstrated by Fujimoto *et al.* (29). Both $Cl^-$ and $Br^-$ ions were reported to have positive effects. Burch *et al.* (30, 31) carried out a series of studies on the effect of chlorine over various catalysts. They found that the pulse injection of gaseous chlorinated compounds over $MnO_2$-based catalysts, lithium-doped MgO, and $Sm_2O_3$ catalysts markedly increased the $C_2$ selectivity. Moffat and coworkers (32, 33) found that the addition of a small amount of tetrachloromethane to the reactant stream could improve the catalytic activity of $La_2O_3$, $Pr_6O_{11}$, and $Sm_2O_3$. They attributed the improvement to oxychloride formation. In recent years, a number of La–Ba–$X$ ($X$ = F, Cl, Br) catalysts have been studied in our laboratory. Catalysts such as $LaF_3/La_2O_3$ (34), $BaBr_2/La_2O_3$ (35), $BaCO_3$/LaOBr (36), $BaCO_3$/LaOCl (37), and $BaCO_3$/LaOF (38) were found to perform well. In this paper, we illustrate how $Y_2O_3$ was promoted by alkaline earth cations and halide anions. We also report how we came to and consequently characterized the 30 mol% $BaCl_2/Y_2O_3$ catalyst using techniques such as GC, XRD, XPS, $O_2$, and $CO_2$ TPD, $^{18}O/^{16}O$ isotope exchange, and TPR.

## EXPERIMENTS

The $MO/Y_2O_3$ ($M$ = Mg, Ca, Sr, Ba) and $BaX_2/Y_2O_3$ ($X$ = Cl, Br) catalysts were prepared by impregnating (with constant heating and stirring to dryness) commercial $Y_2O_3$ (Shanghai Chemicals, purity >99.99%) respectively with a solution of $M(NO_3)_2$ (MERCK, purity >99%) and $BaX_2$. The $BaF_2/Y_2O_3$ catalysts were prepared by grinding the right amounts of $BaF_2$ (Beijing Chemicals, purity >98.6%) with $Y_2O_3$. These catalysts were calcined in air at 800°C for 5 h before being ground, tableted, crushed, and sieved into 40–80 mesh.

The reactions were carried out with 0.5 g of the catalyst in a fix-bed quartz flow microreactor (i.d. = 4 mm) at atmospheric pressure (36). A thermocouple was used to measure the reaction temperatures which were ranging from 600 to 800°C at 50° intervals. Methane (Hong Kong Oxygen Company, purity 99.5%), air, and nitrogen were passed through the microreactor. The flow-rate of each gas was controlled by a mass flow controller and was 8.3 ml min$^{-1}$ for methane, 16 ml min$^{-1}$ for air, and 25.7 ml min$^{-1}$ for nitrogen; giving a contact time of 0.6 g s ml$^{-1}$. The exit flow rate was 50 ml min$^{-1}$ as indicated by a flowmeter. The product distribution was determined by a Shimadzu 8A TCD gas chromatograph with Porapak Q and 5A molecular sieve columns. The measurement for catalytic activity was taken after an on-stream time of 1 h at a particular reaction temperature. The reaction products were $H_2O$, CO, $CO_2$, $C_2H_6$, and $C_2H_4$. As hydrogen was used as the carrier gas, $H_2$ was not detectable as a product. The activity of a catalyst was expressed by means of methane conversion and $C_2$ hydrocarbon selectivity with accuracy estimated to be within 5%. The calculation of methane conversion and selectivity for $C_2$ were based on total carbon balance. A carbon balance of 100 ± 2% was obtained for every run over the catalysts. The conversion of methane or oxygen was defined as

$$c(\mathrm{CH_4 \text{ or } O_2}) = \frac{\text{moles } \mathrm{CH_4} \text{ or } \mathrm{O_2} \text{ converted}}{\text{moles } \mathrm{CH_4} \text{ or } \mathrm{O_2} \text{ fed}} \times 100\%$$

The selectivity for $C_2$ products was calculated as

$$s(\mathrm{C_2}) = \frac{2 \times \text{moles } (\mathrm{C_2H_4 + C_2H_6}) \text{ in products}}{\text{moles } \mathrm{CH_4} \text{ converted to all products}} \times 100\%$$

The yield for $C_2$ product was given by

$$y(\mathrm{C_2}) = c(\mathrm{CH_4}) \times s(\mathrm{C_2}).$$

The specific surface area of the catalysts was measured by the BET method. The continuous flow chromatographic technique was adopted with helium as the carrier gas and nitrogen as the adsorbate. The method was based on the amount of nitrogen adsorbed at low temperature (−196°C) and desorbed at higher temperature. The specific surface areas of the catalysts were calculated according to the BET equation.

The phase composition of catalysts before and after OCM reaction was determined by an X-ray diffractometer (D-MAX, Rigaku) with Cu K$\alpha$ radiation ($\lambda = 1.542$ Å). The pattern obtained was referred to the powder diffraction file—PDF-2 Database for the identification of crystal structures. X-ray photoelectron spectroscopy (XPS, Leybold Heraeus-Shengyang SKL-12) was performed to characterize the catalyst surface, using Mg K$\alpha$ as the X-ray source. The binding energies were calibrated to the C*ls* value of contaminant carbon (284.6 eV). Surface compositions were calculated using the equation

$$\mathrm{X}_i = (\mathrm{A}_i/\mathrm{S}_i) \times 100\Big/\sum(\mathrm{A}_i/\mathrm{S}_i),$$

where $A_i$ is peak area of XPS signal of element $i$ and $S_i$ is the corresponding atomic sensitivity factor.

For the $O_2$ and $CO_2$ TPD studies, 0.2 g of the sample was placed in the middle of a quartz microreactor with 4-mm inner diameter. Silica was located at the bottom of the catalyst bed to reduce the residual space. The gases, after passing through the microreactor, were analyzed online by mass spectrometry (HP G1800A). The heating rate was 15°C $min^{-1}$ and the temperature range was from room temperature to 800°C. Before performing the $O_2$ TPD experiments, the sample was first calcined *in situ* at 800°C for 1 h under an oxygen flow of 15 ml $min^{-1}$, followed by cooling in oxygen to room temperature and helium purging (flow rate = 20 ml $min^{-1}$) for 30 min. In the $CO_2$ TPD experiments, the catalysts were first treated exactly as the $O_2$ TPD experiments before exposure to a flow of $CO_2$ gas (20 ml $min^{-1}$) for 10 min at room temperature followed by helium purging for 20 min.

For the analysis of chlorine content, the catalyst was first digested in 0.1 *M* NaOH solution. The resulting solution was neutralized by 2 *M* $HNO_3$ solution and titrated against standardized $AgNO_3$ solution using 0.005 *M* potassium chromate as indicator (39).

The exchange between gas phase $^{18}O_2$ and surface $^{16}O$ was studied in the temperature range of 100 to 800°C, using a pulse reaction system with a pulse size of 1.12 $\mu$mol. Catalyst (ca 0.2 g) was placed in a tubular quartz flow reactor (i.d. 4 mm) and was treated with pure $O_2$ and $N_2$ (0.5 h each; flow rate = 50 ml $min^{-1}$) at 800°C; $^{18}O_2$ was then pulsed over the catalyst at the desired temperature. The effluent from the reactor was directed to a GC-MS (HP G1800A GCD) system for analysis.

Temperature-programmed reduction (TPR) was conducted by using a 7% $H_2$–93% $N_2$ (v/v) mixture. The flow rate of the carrier gas was 50 ml $min^{-1}$ and a thermal conductivity detector was used; 0.2 g of sample was used and the heating rate was 10°C $min^{-1}$.

The reducible oxygen studies were also performed on the MS (HP G1800A) system. The pulse size of $O_2$ was 65.7 $\mu$L (at 25°C, 1 atm). The catalyst (0.2 g) was placed in a quartz reactor and was first reduced in $H_2$ at the desired temperature for 1 h, followed by $O_2$-pulsing at 800°C. We kept on pulsing $O_2$ over the reduced sample until after passing the catalyst, there was no observable decrease in $O_2$-pulse size. The total amount of $O_2$ absorbed by the catalyst was then estimated and expressed in mole per gram of catalyst.

## RESULTS

### *Catalytic Performance of $Y_2O_3$ and MO (M = Mg, Ca, Sr, Ba)-Promoted $Y_2O_3$ Catalysts*

Table 1 shows the catalytic activities of the 30 mol% *M*O/$Y_2O_3$ catalysts. It is clear that the addition of 30 mol% of CaO, SrO, and BaO to $Y_2O_3$ has significantly enhanced the conversion of $CH_4$ and the selectivity to $C_2$. As a result, compared to $Y_2O_3$, the $C_2$ yield of the promoted $Y_2O_3$ catalysts was nearly double. One can also see enhancement in the rate of $CH_4$ reaction. Comparing the four 30 mol% *M*O/$Y_2O_3$ catalysts, the SrO- and BaO-promoted ones performed better than the CaO- and MgO-promoted catalysts. The performance of the catalysts goes along the series: $Y_2O_3 \approx$ 30 mol% MgO/$Y_2O_3 <$ 30 mol% CaO/$Y_2O_3 <$ 30 mol% SrO/$Y_2O_3 \approx$ 30 mol% BaO/$Y_2O_3$. The 30 mol% BaO/$Y_2O_3$ catalyst is slightly superior to the 30 mol% SrO/$Y_2O_3$ one, as the former performed better at lower temperatures (650 and 700°C). For the pure BaO, the $C_2$ yield was poor below 750°C, but at 800°C its performance was matching that of the 30 mol% BaO/$Y_2O_3$ catalyst. Since the 30 mol% BaO/$Y_2O_3$ catalyst was the best among the *M*O-promoted $Y_2O_3$ catalysts, we chose to modify the Y–Ba catalyst with halogens with the hope to achieve even better performance.

### *Catalytic Performance of $BaX_2$ (X = F, Cl, Br)-Promoted $Y_2O_3$ Catalysts*

First we investigated the effects of halide ions. $BaF_2$, $BaCl_2$, and $BaBr_2$ were used instead of BaO for the modification of $Y_2O_3$. From Table 2, one can see that all the Ba$X_2$-promoted catalysts are good-performance catalysts. At 750 and 800°C, $C_2$ yields of ca 20–22.5% were achieved over the 30 mol% $BaF_2$/$Y_2O_3$ and 30 mol% $BaCl_2$/$Y_2O_3$ catalysts, with the latter being slightly superior to the former. Over the 30 mol% $BaBr_2$/$Y_2O_3$ catalyst, the $C_2$ yield was 18.6% at 750°C. Figure 1 gives a comparison of the $Y_2O_3$, 30 mol% BaO/$Y_2O_3$, and 30 mol% Ba$X_2$/$Y_2O_3$ catalysts. Compared to a 30 mol% BaO/$Y_2O_3$ catalyst, the Ba$X_2$-promoted $Y_2O_3$ catalysts can give better $C_2$ selectivities (improved from ca 40 to 50%) above 700°C. There were slight decreases in $CH_4$ conversions over the $BaF_2$- and $BaBr_2$-promoted $Y_2O_3$ catalysts. Over the 30 mol% $BaCl_2$/$Y_2O_3$ catalyst, however, $CH_4$ conversion was slightly higher than the 30 mol% BaO/$Y_2O_3$ catalyst. As far as the $C_2$ yield is concerned, all the Ba$X_2$-promoted catalysts performed better than the BaO-promoted one at 750 and 800°C. For pure $BaCl_2$, the $C_2$ yield was poor below 750°C. At 800°C, it was 14.6%.

### *Effects of $BaCl_2$ and BaO Loadings on the BaO/$Y_2O_3$ and $BaCl_2$/$Y_2O_3$ Catalysts*

Figure 2 shows that as the loadings of BaO increased from 0 to 50 mol% in the BaO/$Y_2O_3$ catalysts, the conversion of methane increased from ca 30 to 47% at OCM reaction temperatures of 750 and 800°C. Over the $BaCl_2$/$Y_2O_3$ catalysts, methane conversion increased rather similarly from 0 to 30 mol% $BaCl_2$ loadings. Between 40 and 50 mol%, there was a drop (ca 4%) in methane conversion. One can see that with the addition of $BaCl_2$ to $Y_2O_3$, $C_2$ selectivity was greatly enhanced (from ca 26 to 55%). For the BaO-promoted catalysts, $C_2$ selectivity was ranging from ca 22 to 50%. The $BaCl_2$/$Y_2O_3$ catalysts are outstandingly superior to the BaO/$Y_2O_3$ catalysts in $C_2$ selectivity between the range of 0 to 40 mol% loadings. At 50 mol%, the $C_2$ selectivities over the two catalysts were rather close. Actually, at 50 mol% loadings, the BaO/$Y_2O_3$ catalyst performed better

**TABLE 1**

**The Catalytic Performance of $Y_2O_3$ and $M$O ($M$ = Mg, Ca, Sr, Ba)-Promoted $Y_2O_3$ Catalysts**

| Catalyst | $T$ (°C) | Conversion (%) | | | Selectivity (%) | | | $C_2$ yield (%) | Rate of $CH_4$ reaction ($10^{17}$ molecules $m^{-2}$ $s^{-1}$) |
|---|---|---|---|---|---|---|---|---|---|
| | | $CH_4$ | $O_2$ | $CO_x$ | $C_2H_4$ | $C_2H_6$ | $C_2$ | | |
| $Y_2O_3$ | 600 | 25.0 | 89.0 | 88.5 | 4.80 | 6.70 | 11.5 | 3.00 | 0.46 |
| | 650 | 25.9 | 89.5 | 84.7 | 7.90 | 7.40 | 15.3 | 4.00 | 0.46 |
| | 700 | 26.8 | 91.5 | 79.1 | 13.3 | 7.60 | 20.9 | 5.60 | 0.47 |
| | 750 | 30.3 | 92.8 | 73.8 | 18.0 | 8.20 | 26.2 | 7.80 | 0.53 |
| | 800 | 31.8 | 92.0 | 73.1 | 16.3 | 8.60 | 26.9 | 8.60 | 0.56 |
| $MgO/Y_2O_3$ | 600 | 23.0 | 82.0 | 84.6 | 7.70 | 7.70 | 15.4 | 3.50 | 0.40 |
| | 650 | 24.1 | 88.0 | 76.4 | 14.2 | 9.40 | 23.6 | 5.70 | 0.42 |
| | 700 | 26.6 | 87.5 | 70.6 | 18.9 | 10.5 | 29.4 | 7.80 | 0.46 |
| | 750 | 27.2 | 90.0 | 70.0 | 20.0 | 10.0 | 30.0 | 8.10 | 0.48 |
| | 800 | 24.8 | 88.0 | 75.2 | 17.7 | 7.10 | 24.8 | 6.20 | 0.43 |
| $CaO/Y_2O_3$ | 600 | 34.1 | 87.2 | 71.9 | 13.8 | 15.3 | 28.1 | 9.60 | 0.75 |
| | 650 | 38.9 | 91.0 | 64.0 | 21.0 | 15.0 | 36.0 | 14.0 | 0.86 |
| | 700 | 37.4 | 90.0 | 59.3 | 23.7 | 17.0 | 40.7 | 15.2 | 0.82 |
| | 750 | 38.9 | 97.6 | 63.9 | 22.2 | 13.9 | 36.1 | 14.0 | 0.86 |
| | 800 | 36.7 | 98.0 | 70.9 | 20.8 | 8.30 | 29.1 | 10.7 | 0.81 |
| $SrO/Y_2O_3$ | 600 | 28.1 | 75.0 | 81.3 | 7.00 | 12.7 | 18.7 | 5.30 | 0.93 |
| | 650 | 36.0 | 93.0 | 66.7 | 18.2 | 15.1 | 33.3 | 12.0 | 1.20 |
| | 700 | 38.5 | 96.0 | 56.9 | 27.1 | 16.0 | 43.1 | 16.6 | 1.30 |
| | 750 | 38.6 | 96.1 | 56.7 | 28.4 | 14.9 | 43.3 | 16.7 | 1.30 |
| | 800 | 36.6 | 97.0 | 62.4 | 28.2 | 9.40 | 37.6 | 13.8 | 1.20 |
| $BaO/Y_2O_3$ | 650 | 42.3 | 90.0 | 60.0 | 23.4 | 16.6 | 40.0 | 16.8 | 1.40 |
| | 700 | 43.2 | 96.2 | 60.6 | 21.5 | 17.9 | 39.4 | 17.0 | 1.43 |
| | 750 | 39.7 | 97.5 | 60.5 | 23.0 | 16.5 | 39.5 | 15.7 | 1.31 |
| | 800 | 39.1 | 97.7 | 68.7 | 20.1 | 11.2 | 31.3 | 12.2 | 1.29 |
| Pure BaO | 650 | 1.00 | 4.00 | 100 | 0.00 | 0.00 | 0.00 | 0.00 | 0.01 |
| | 700 | 3.00 | 19.2 | 58.8 | 0.00 | 41.2 | 41.2 | 0.00 | 0.31 |
| | 750 | 10.1 | 28.1 | 37.3 | 22.2 | 40.5 | 62.7 | 6.30 | 1.05 |
| | 800 | 21.2 | 69.0 | 40.8 | 32.9 | 26.3 | 59.2 | 12.6 | 2.21 |

*Note*. The loading of $M$O on $Y_2O_3$ was 30 mol%. $CH_4:O_2:N_2$, 2.47 : 1 : 11.4. The total flow rate was 50 ml $min^{-1}$. Contact time, 0.6 g s $ml^{-1}$. The weight of catalyst was 0.5 g.

than the $BaCl_2/Y_2O_3$ catalyst. $C_2$ yields of ca 24% were achieved at 750 and 800°C. Over the 50 mol% $BaCl_2/Y_2O_3$, they were ca 17 and 21% respectively at 750 and 800°C. The $C_2$ yield obtained over the 40 mol% $BaO/Y_2O_3$ and the 40 mol% $BaCl_2/Y_2O_3$ catalysts were rather similar, around 21%. Below 40 mol%, the $BaCl_2/Y_2O_3$ catalysts definitely out-performed the $BaO/Y_2O_3$ catalysts.

### *BET, XRD, and XPS Studies*

Figure 3 reveals that the specific surface areas of the $BaCl_2/Y_2O_3$ catalysts decreased as the $BaCl_2$ loadings increased. Between 0 and 30 mol% $BaCl_2$ loadings, the specific surface areas of the fresh $BaCl_2/Y_2O_3$ catalysts decreased from ca 10.4 to 5.6 $m^2$ $g^{-1}$. There was another decrease of ca 1.0 $m^2$ $g^{-1}$ from 20 to 50 mol%. For the catalysts used in OCM reactions at 800°C, the specific surface areas became even smaller. The value for the used $Y_2O_3$ catalyst was ca 7.0 $m^2$ $g^{-1}$. For the used 40 and 50 mol% $BaCl_2/Y_2O_3$ catalysts, the specific surface areas were ca 1.3 $m^2$ $g^{-1}$. Similarly, a fresh 30 mol% $BaO/Y_2O_3$ catalyst has a specific surface area of ca 6.0 $m^2$ $g^{-1}$ before OCM reaction. After OCM reaction at 800°C, it was ca 3.9 $m^2$ $g^{-1}$. Hence, with the increase in BaO or $BaCl_2$ loadings on $Y_2O_3$, there was reduction in specific surface area. In general, the specific surface areas of the catalysts reduced further during OCM reactions.

XRD investigations revealed that for the fresh 30 mol% $BaO/Y_2O_3$ catalyst, there were weak signals of orthorhombic BaO and $BaCO_3$ along with the cubic $Y_2O_3$ signals. For the fresh 30 mol% $BaCl_2/Y_2O_3$ catalyst, only $Y_2O_3$ signals were detected. However, after OCM reaction, weak signals due to orthorhombic $Ba_3Cl_4CO_3$ and $BaCO_3$ were observed. Based on detailed XRD investigations, we know that the size of the $Y_2O_3$ lattice increased as the BaO and $BaCl_2$ loadings of the $BaO/Y_2O_3$ and $BaCl_2/Y_2O_3$ catalysts increased (Fig. 4). The crystal structure of $Y_2O_3$ is of the fluoride type (40). The length ($a_0$) of the unit cell edge is 10.604 Å. For the fresh $BaO/Y_2O_3$ catalysts, $a_0$ increased only slightly with the increase of BaO loadings from 0 to 40 mol%. At 50 mol%, $a_0$ was 10.613 Å. After the OCM

**TABLE 2**

**The Catalytic Performance of Ba$X_2$ ($X$ = F, Cl, Br)-Promoted $Y_2O_3$ Catalysts**

| Catalyst | $T$ (°C) | Conversion (%) $CH_4$ | Conversion (%) $O_2$ | Conversion (%) $CO_x$ | Selectivity (%) $C_2H_4$ | Selectivity (%) $C_2H_6$ | Selectivity (%) $C_2$ | $C_2$ yield (%) | Rate of $CH_4$ reaction ($10^{17}$ molecules $m^{-2}$ $s^{-1}$) |
|---|---|---|---|---|---|---|---|---|---|
| $BaF_2/Y_2O_3$ | 650 | 12.9 | 64.4 | 79.1 | 6.30 | 14.6 | 20.9 | 2.70 | 0.98 |
| | 700 | 30.6 | 80.1 | 62.1 | 20.4 | 17.5 | 37.9 | 11.6 | 2.33 |
| | 750 | 38.2 | 91.4 | 53.4 | 29.9 | 16.7 | 46.6 | 17.8 | 2.91 |
| | 800 | 39.0 | 93.3 | 49.6 | 33.3 | 17.1 | 50.4 | 19.7 | 2.97 |
| $BaCl_2/Y_2O_3$ | 650 | 19.8 | 33.9 | 67.9 | 13.3 | 18.8 | 32.1 | 6.30 | 0.59 |
| | 700 | 32.3 | 67.3 | 55.6 | 25.6 | 18.8 | 44.4 | 14.3 | 0.97 |
| | 750 | 40.6 | 86.5 | 49.7 | 36.7 | 13.6 | 50.3 | 20.5 | 1.22 |
| | 800 | 43.2 | 92.9 | 48.3 | 39.7 | 12.0 | 51.7 | 22.3 | 1.31 |
| $BaBr_2/Y_2O_3$ | 650 | 31.0 | 82.1 | 63.9 | 25.8 | 10.3 | 36.1 | 11.2 | 0.71 |
| | 700 | 36.7 | 93.1 | 54.9 | 36.5 | 8.60 | 45.1 | 16.5 | 0.84 |
| | 750 | 38.2 | 94.1 | 51.4 | 41.3 | 7.30 | 48.6 | 18.6 | 0.87 |
| | 800 | 35.7 | 94.3 | 52.7 | 37.2 | 10.1 | 47.3 | 16.9 | 0.82 |
| Pure $BaCl_2$ | 650 | 0.74 | 3.00 | 30.2 | 0.00 | 69.8 | 69.8 | 0.52 | 0.03 |
| | 700 | 1.73 | 6.00 | 26.1 | 0.00 | 73.8 | 73.8 | 1.28 | 0.06 |
| | 750 | 5.14 | 15.0 | 17.6 | 25.2 | 57.2 | 82.4 | 4.24 | 0.19 |
| | 800 | 17.5 | 35.1 | 16.5 | 56.6 | 26.9 | 83.5 | 14.6 | 0.54 |

*Note.* The loading of Ba$X_2$ was 30 mol%. The reaction conditions were the same as those in Table 1.

reaction, the $BaO/Y_2O_3$ catalysts showed much larger $a_0$ values. It was ca 10.620 Å at 30, 40, and 50 mol% loadings. For the fresh $BaCl_2/Y_2O_3$ catalysts, the $a_0$ values increased gradually from 10.604 to ca 10.627 Å as the $BaCl_2$ loadings increased from 0 to 50 mol%. After OCM reaction, $a_0$ increased to ca 10.638 Å.

For the $BaCl_2/Y_2O_3$ catalyst, the Ba3$d_{5/2}$ and Cl2$p$ peaks were at ca 781.0 and 199.0 eV binding energies, respectively. The Y3$d$ peak was at ca 158.0 eV. Based on the XPS peak areas and the atomic sensitivity factors of the elements, the elemental compositions on the surfaces of the fresh and used 30 mol% $BaCl_2/Y_2O_3$ catalyst were calculated (Table 3). There was a distinct decrease in Ba/Y ratio after 12 h of the OCM reaction. There was no significant change in surface chlorine composition during the OCM reaction. Similar results (not shown) were obtained over the 10 and 50 mol% $BaCl_2/Y_2O_3$ catalysts.

### *Performance of 30 mol% $BaCl_2/Y_2O_3$ as Related to Reaction Time, Contact Time and $CH_4/O_2$ Ratio*

The 30 mol% $BaCl_2/Y_2O_3$ (0.5 g) was found to be rather stable within a reaction time of 40 h (Fig. 5). At 750°C, with $CH_4 : O_2 : N_2 = 2.47 : 1 : 11.4$ and contact time = 0.6 g s $ml^{-1}$, the $CH_4$ conversion, $C_2$ selectivity, and $C_2$ yield stayed around 41, 51, and 21%, respectively. The $C_2H_4/C_2H_6$ ratio remained at 2.6 within the 40 h of testing time. However, the catalyst was losing chlorine during the reaction. At 4, 8, 12, 16, and 20 h, the losses of chlorine were around 3.5, 8.3, 13.5, 13.6, and 15.5% of the original amount. Apparently, the loss of ca 15.5% of chlorine from the 30 mol% $BaCl_2/Y_2O_3$ catalyst has little effect on the performance of the catalyst.

**TABLE 3**

**Surface Elemental Composition of the 30 mol% $BaCl_2/Y_2O_3$ Catalyst before and after OCM Reaction of 12 h, Based on the XPS Data**

| | Ba (%) | Cl (%) | Y (%) | O (%) | C (%) | Ba/Y |
|---|---|---|---|---|---|---|
| Before | 6.0 | 11.5 | 24.7 | 47.6 | 10.7 | 0.24 |
| 12 h | 1.6 | 11.5 | 26.2 | 39.0 | 21.8 | 0.06 |

At 750°C and with a contact time of 0.36 g s $ml^{-1}$, the variation of the $CH_4/O_2$ ratio from 1 to 5 would cause the $CH_4$ conversion and the $C_2H_4/C_2H_6$ ratio to drop from ca 75 to 29% and from ca 4.5 to 1.4, respectively (Fig. 6a). The $C_2$ selectivity increased from ca 10.6 to 60.0%. The $C_2$ yield was ca 12% at $CH_4/O_2 = 1$ and reached 19.5% at $CH_4/O_2 = 2$, and then slightly decreased to reach ca 18% at $CH_4/O_2 = 5$.

Figure 6b shows that at 750°C and with $CH_4/O_2 = 2.47$, as the contact time increased from 0.06 to 0.86 g s $ml^{-1}$, $CH_4$ conversion and $C_2H_4/C_2H_6$ ratio increased from ca 13 to 41% and from 0.7 to 2.7, respectively. The $C_2$ selectivity, however, decreased from ca 57 to 40%. When the contact time was at or above 0.12 g s $ml^{-1}$, the $C_2$ yield stayed around 19%. The effect of changing the contact time between 0.2 and 0.7 g s $ml^{-1}$ on the $C_2$ yield was not significant.

### *$O_2$ and $CO_2$ TPD Studies of $BaO/Y_2O_3$ and $BaCl_2/Y_2O_3$*

Figure 7 shows the $O_2$ TPD spectra of the fresh 0–50 mol% $BaO/Y_2O_3$ catalysts. For comparison, the $O_2$ TPD

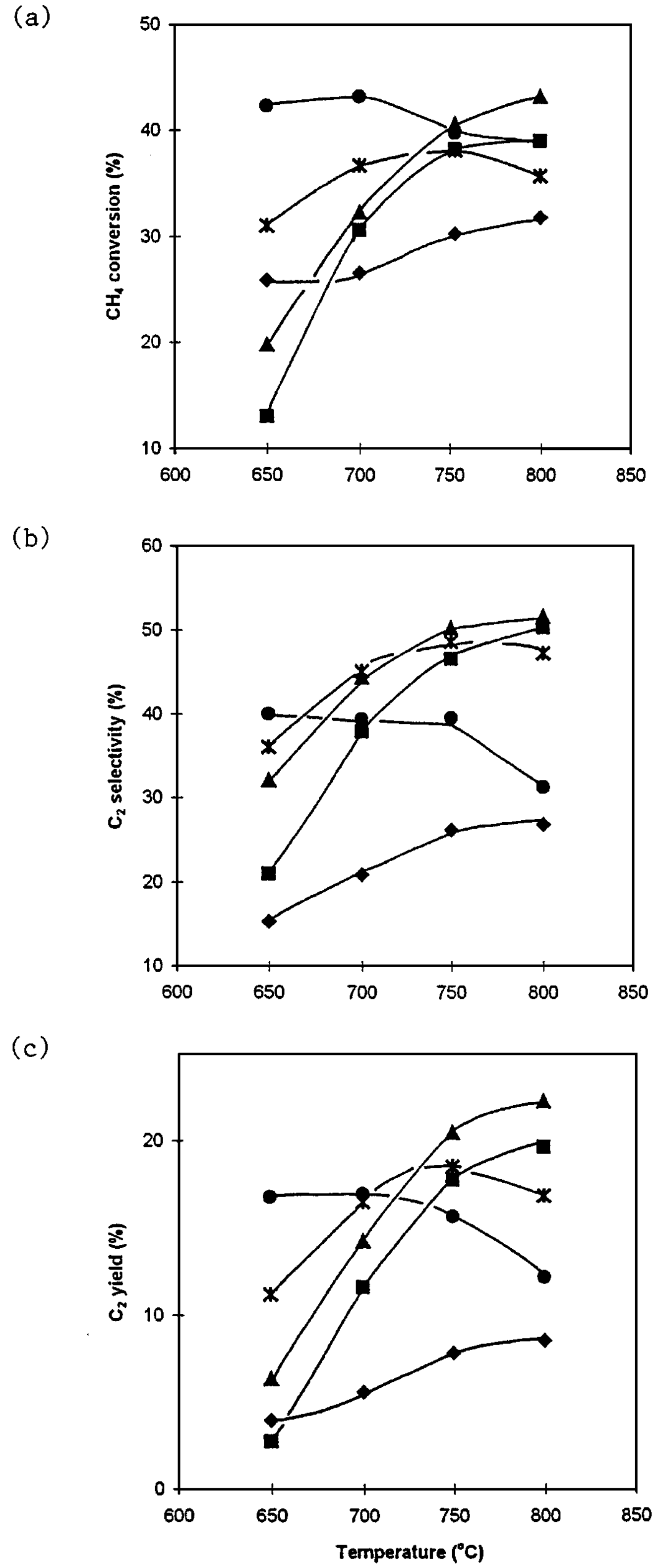

**FIG. 1.** Comparison of the catalytic performance of the $Y_2O_3$ (◆), 30 mol% $BaO/Y_2O_3$ (●), 30 mol% $BaF_2/Y_2O_3$ (■), 30 mol% $BaCl_2/Y_2O_3$ (▲), and 30 mol% $BaBr_2/Y_2O_3$ (∗) catalysts: (a) $CH_4$ conversion; (b) $C_2$ selectivity; and (c) $C_2$ yield. Reaction conditions were the same as those in Table 1.

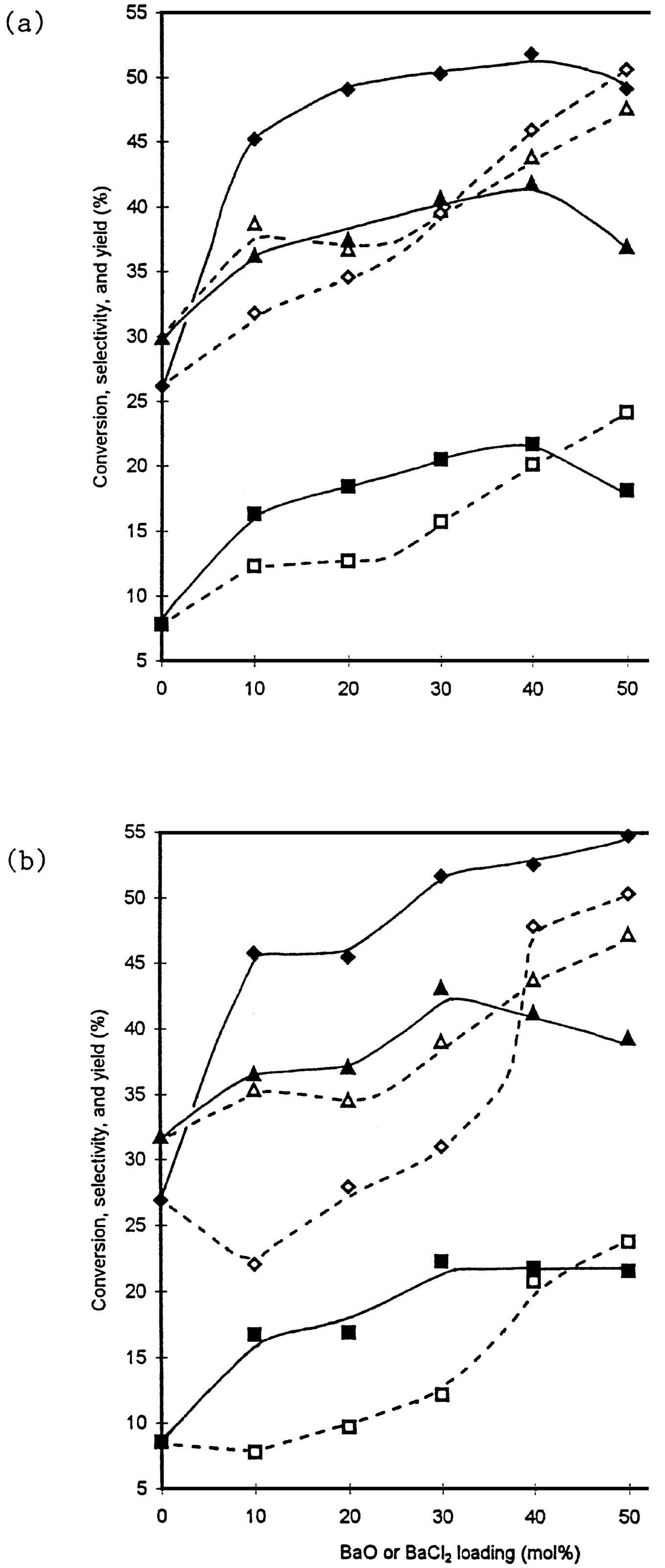

**FIG. 2.** The catalytic performance of 30 mol% $BaO/Y_2O_3$ (hollow symbols) and 30 mol% $BaCl_2/Y_2O_3$ (solid symbols) catalysts at (a) 750 and (b) 800°C as related to BaO and $BaCl_2$ loadings: (△) $CH_4$ conversion; (◇) $C_2$ selectivity; and (□) $C_2$ yield.

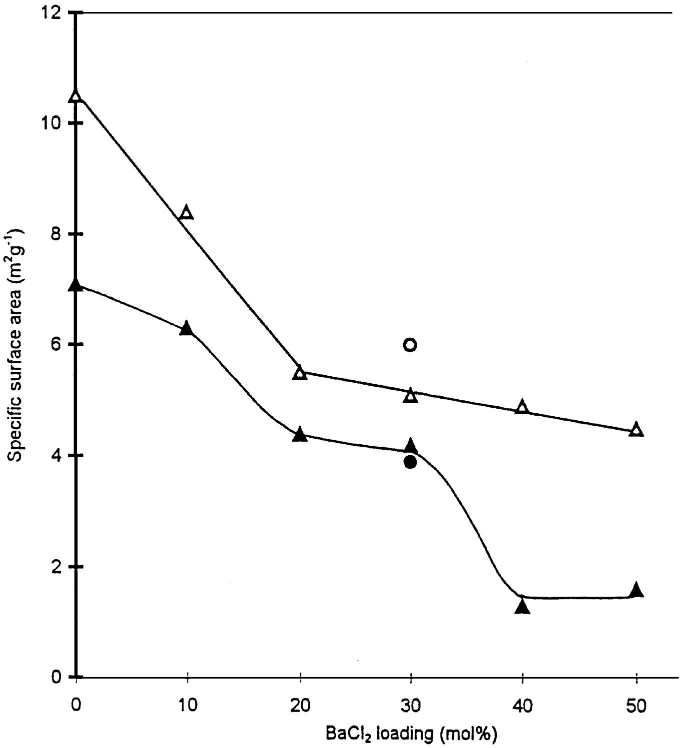

**FIG. 3.** The specific surface areas of BaCl$_2$/Y$_2$O$_3$ (△) catalysts before (hollow symbols) and after (solid symbols) OCM reactions at 800°C as related to BaCl$_2$ loading. Also shown for comparison are the specific surface areas of the 30 mol% BaO/Y$_2$O$_3$ (○) catalyst.

spectrum of a 30 mol% BaO/Y$_2$O$_3$ catalyst used in OCM reaction was also presented (Fig. 7d′). With no BaO, Y$_2$O$_3$ gave an O$_2$ TPD peak at 400°C. The amount of O$_2$ desorbed was ca $0.07 \times 10^{-5}$ mol g$^{-1}$. With the additions of 10 and 20 mol% BaO, this peak increased in intensity and at 30 mol% BaO loading, a shoulder was clearly developed at 480°C. The O$_2$ TPD profile of a 30 mol% BaO/Y$_2$O$_3$ catalyst used in OCM reaction is very similar to that of a fresh 30 mol% BaO/Y$_2$O$_3$ catalyst. The total O$_2$ desorbed was ca $3.7 \times 10^{-5}$ mol g$^{-1}$. At 40 and 50 mol% BaO loadings, the O$_2$ TPD spectrum showed a broad peak centred at ca 480°C. The intensities of the O$_2$ TPD peaks increased further with the increase in BaO loading.

For the fresh 0–70 mol% BaCl$_2$/Y$_2$O$_3$ catalysts, the O$_2$ TPD peaks shifted gradually from 400 to ca 480°C. The intensities of the peaks decreased as the loading of BaCl$_2$ increased (Fig. 8). The amount of O$_2$ desorbed from a fresh 30 mol% BaCl$_2$/Y$_2$O$_3$ catalyst was ca $0.04 \times 10^{-5}$ mol g$^{-1}$. For a 30 mol% BaCl$_2$/Y$_2$O$_3$ catalyst used in OCM reaction for 4 h, another peak at ca 350°C developed besides the 450°C peak (Fig. 9). After 8 or 12 h of OCM reaction, the O$_2$ TPD profile showed two components at ca 367 and 461°C. Such O$_2$ TPD profile appeared to be quite similar to that obtained over a 30 mol% BaO/Y$_2$O$_3$ catalyst used in OCM reaction (Fig. 7d′). The amount of O$_2$ desorbed was around $0.11 \times 10^{-5}$ mol g$^{-1}$. The results imply that in the course of the OCM reaction, a 30 mol% BaCl$_2$/Y$_2$O$_3$ catalyst was changing in nature and was developing a character that resembled a 30 mol% BaO/Y$_2$O$_3$ catalyst.

Such notion is supported by the CO$_2$ TPD results obtained over the 30 mol% BaO/Y$_2$O$_3$ and 30 mol% BaCl$_2$/Y$_2$O$_3$ catalysts. For the CO$_2$ TPD profile obtained over a fresh Y$_2$O$_3$ catalyst, there were peaks at ca 100, 140, and 335°C and shoulders at 175 and 500°C (Fig. 10). Clearly, there were basic sites of various strength existed on the surface. For a fresh 30 mol% BaO/Y$_2$O$_3$ catalyst, only weak peaks were observed at 90 and 140°C; implying the catalyst was low in surface basicity. CO$_2$ desorption was observed above 650°C, possibly due to the decomposition of surface carbonate species. For a fresh 30 mol% BaCl$_2$/Y$_2$O$_3$ catalyst, peaks were observed at 100 and 140°C and a large broad band at 500°C. However, after OCM reaction, the 30 mol% BaCl$_2$/Y$_2$O$_3$ catalyst exhibited a profile very similar to that of a fresh 30 mol% BaO/Y$_2$O$_3$ catalyst: there were small CO$_2$ desorption peaks at ca 100 and 188°C and large desorption above 600°C. In other words, during OCM reaction, the 30 mol% BaCl$_2$/Y$_2$O$_3$ catalyst was changing into somewhat like a 30 mol% BaO/Y$_2$O$_3$ catalyst, with the lowering in surface basicity being observed.

### *$^{18}$O/$^{16}$O Isotope Exchange over Y$_2$O$_3$, 30 mol% BaO/Y$_2$O$_3$, and 30 mol% BaCl$_2$/Y$_2$O$_3$*

Figure 11b reveals that the exchange of $^{18}$O and $^{16}$O was most efficient over the 30 mol% BaO/Y$_2$O$_3$ catalyst. Single exchange product $^{18}$O$^{16}$O came to a maximuim

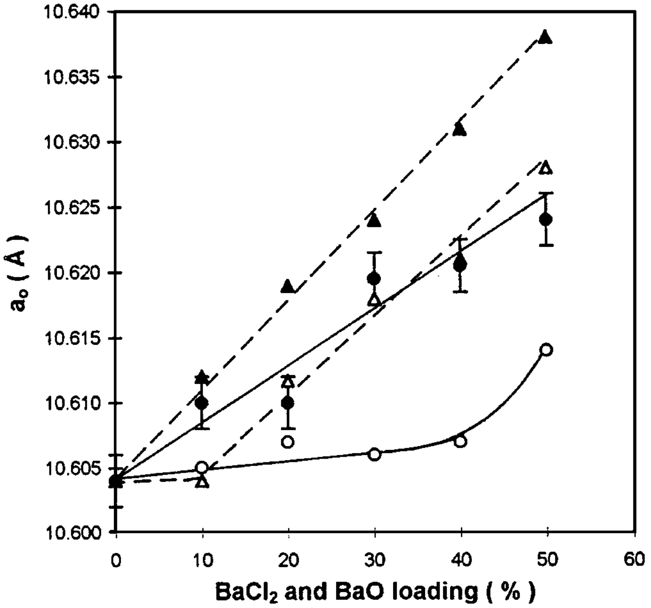

**FIG. 4.** The change of the lattice parameter, $a_0$, of Y$_2$O$_3$ in BaO/Y$_2$O$_3$ (○) and BaCl$_2$/Y$_2$O$_3$ (△) catalysts before (hollow symbols) and after (solid symbol) OCM reaction at 800°C as related to BaO and BaCl$_2$ loadings.

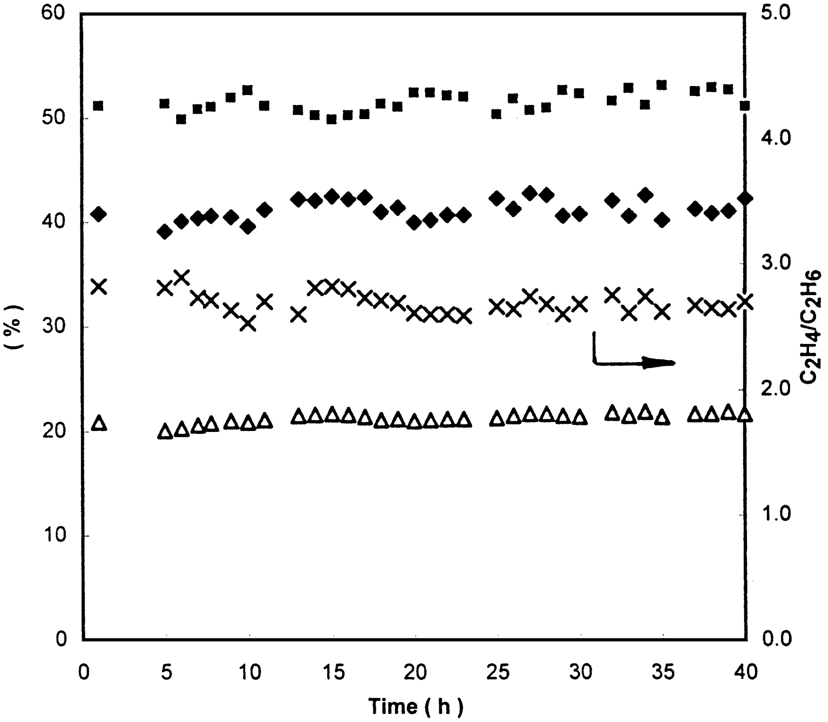

**FIG. 5.** Life study of the 30 mol% $BaCl_2/Y_2O_3$ catalyst at 750°C: (◆) $CH_4$ conversion; (■) $C_2$ selectivity; (△) $C_2$ yield; and (×) $C_2H_4/C_2H_6$ ratio.

at 383°C and complete $^{16}O_2$ production was observed at 504°C. Over $Y_2O_3$, the respective temperatures were at 640 and 778°C (Fig. 11a). Over the 30 mol% $BaCl_2/Y_2O_3$ catalyst, they were at 600 and 745°C (Fig. 11c). Based on these $^{18}O/^{16}O$ isotope exchange results, one can conclude that the rates of $^{18}O/^{16}O$ exchange over the three catalysts decreased in the order of 30 mol% $BaO/Y_2O_3 \gg$ 30 mol% $BaCl_2/Y_2O_3 > Y_2O_3$.

### *Reduction Studies of $Y_2O_3$, 30 mol% $BaO/Y_2O_3$, and 30 mol% $BaCl_2/Y_2O_3$*

Temperature programmed reduction results of the three catalysts are shown in Fig. 12. For the $Y_2O_3$ catalyst within the range of 100 to 800°C, reduction was not significant. For the 30 mol% $BaO/Y_2O_3$ catalyst, reduction occurred at ca 400°C and there was a band at 480°C and above 600°C, reduction was very significant. As for a 30 mol% $BaCl_2/Y_2O_3$ catalyst, reduction occurred at ca 500°C and a band centred at ca 610°C existed. It is clear that reduction was continuing above 750°C. After OCM reaction of 8 h, the TPR profile of a 30 mol% $BaCl_2/Y_2O_3$ catalyst showed a broad band stretching from 480 to well above 800°C.

In order to estimate the amount of reducible oxygen existed in the three catalysts, the catalysts were first reduced in $H_2$ at a desired temperature and then pulses of $O_2$ were passed through the catalysts at 800°C. From the amount of $O_2$ absorbed over each catalyst, one can measure indirectly the amount of oxygen removed in $H_2$-reduction. The idea was based on the assumption that the vacancies generated in $H_2$-reduction will be eventually occupied by oxygen ions during $O_2$ pulsing. Table 4 shows the amount of absorbed $O_2$ at 800°C before the occurrence of zero diminution in $O_2$ pulse size over the three catalysts. It is clear that the amount of reducible oxygen in the 30 mol% $BaO/Y_2O_3$ catalyst was much higher than those in the other two catalysts. Compared to a fresh catalyst, the used 30 mol% $BaCl_2/Y_2O_3$ catalyst contained more reducible oxygen. The threshold temperatures for reduction to occur over the 30 mol% $BaO/Y_2O_3$, 30 mol% $BaCl_2/Y_2O_3$, and $Y_2O_3$ catalysts were respectively ca 400, 600, and 700°C.

**TABLE 4**

**The Amount of Oxygen Absorbed at 800°C over the $Y_2O_3$, 30 mol% $BaO/Y_2O_3$ and 30 mol% $BaCl_2/Y_2O_3$ Catalysts $H_2$-Reduced at Various Temperatures**

| Temperature (°C) | $Y_2O_3$ ($10^{-6}$ mol $g^{-1}$) | 30 mol% $BaO/Y_2O_3$ ($10^{-6}$ mol $g^{-1}$) | 30 mol% $BaCl_2/Y_2O_3$ ($10^{-6}$ mol $g^{-1}$) | 30 mol% $BaCl_2/Y_2O_3$[a] ($10^{-6}$ mol $g^{-1}$) |
|---|---|---|---|---|
| 300 | 0.0 | 0.0 | 0.0 | 0.0 |
| 400 | 0.0 | 0.94 | 0.0 | 0.17 |
| 500 | 0.0 | 3.56 | 0.0 | 0.39 |
| 600 | 0.0 | 4.38 | 0.16 | 0.62 |
| 700 | 0.41 | 6.53 | 0.73 | 0.79 |
| 750 | 0.65 | 6.57 | 1.30 | 1.39 |
| 800 | 1.69 | 7.71 | 1.76 | 2.59 |

[a] After OCM reaction of 8 h.

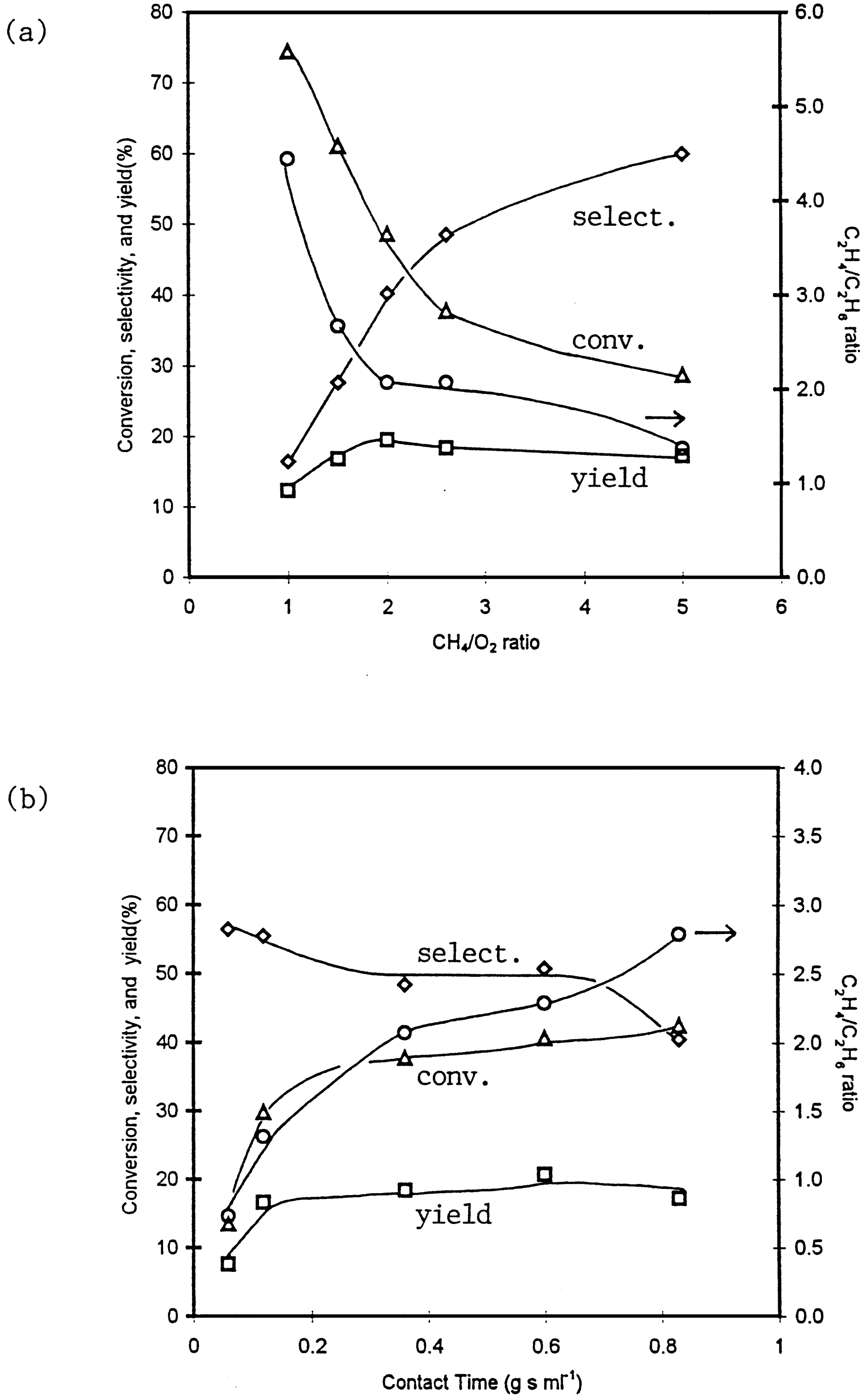

**FIG. 6.** The catalytic performance of a 30 mol% $BaCl_2/Y_2O_3$ catalyst (0.3 g) at 750°C as related to (a) $CH_4/O_2$ ratio (contact time fixed at 0.36 g s $ml^{-1}$) and (b) contact time ($CH_4 : O_2 : N_2$ fixed at 2.47 : 1 : 11.4): (△) $CH_4$ conversion; (◇) $C_2$ selectivity; (□) $C_2$ yield; and (○) $C_2H_4/C_2H_6$ ratio.

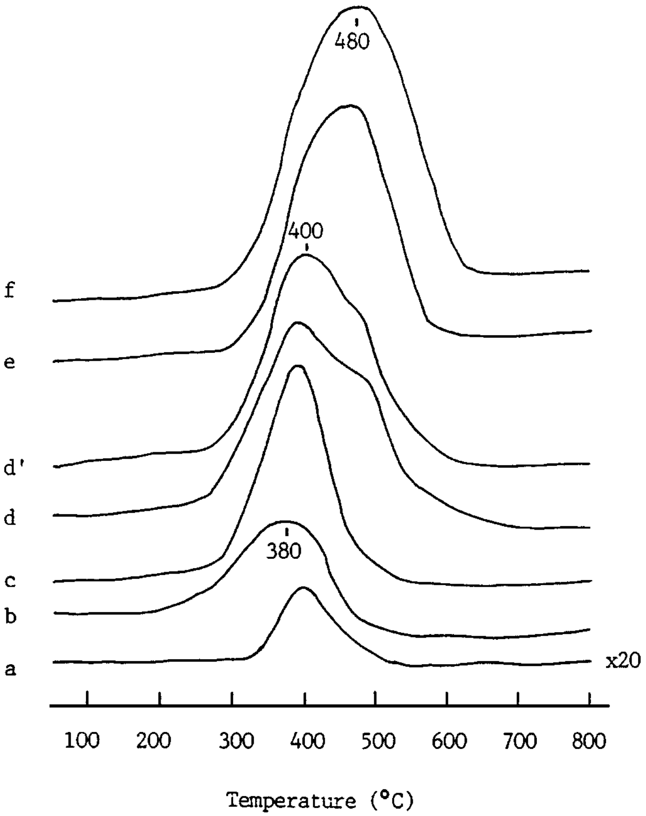

**FIG. 7.** $O_2$ TPD spectra of (a) $Y_2O_3$, (b) 10 mol% $BaO/Y_2O_3$, (c) 20 mol% $BaO/Y_2O_3$, (d) 30 mol% $BaO/Y_2O_3$, (e) 40 mol% $BaO/Y_2O_3$, and (f) 50 mol% $BaO/Y_2O_3$ catalysts before OCM reaction. Also shown (d′) for comparison is the $O_2$ TPD spectrum of a 30 mol% $BaO/Y_2O_3$ catalyst after 8 h in OCM reaction at 800°C.

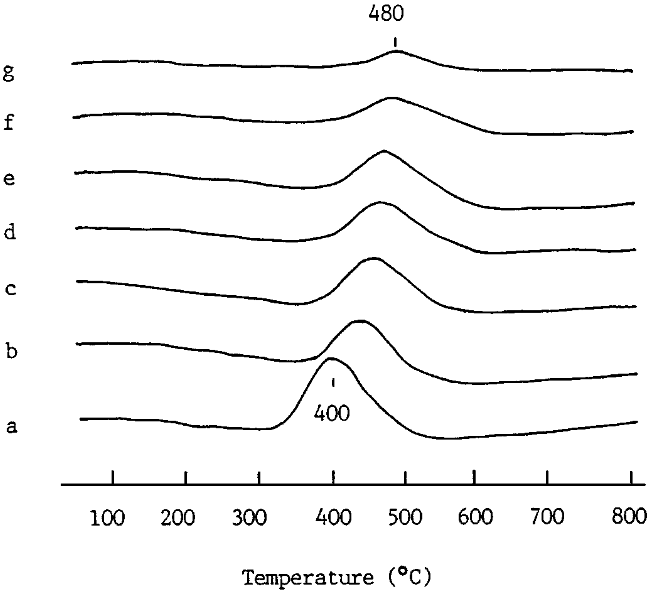

**FIG. 8.** $O_2$ TPD spectra of (a) $Y_2O_3$, (b) 10 mol% $BaCl_2/Y_2O_3$, (c) 20 mol% $BaCl_2/Y_2O_3$, (d) 30 mol% $BaCl_2/Y_2O_3$, (e) 40 mol% $BaCl_2/Y_2O_3$, (f) 50 mol% $BaCl_2/Y_2O_3$, and (g) 70 mol% $BaCl_2/Y_2O_3$ catalysts before OCM reaction.

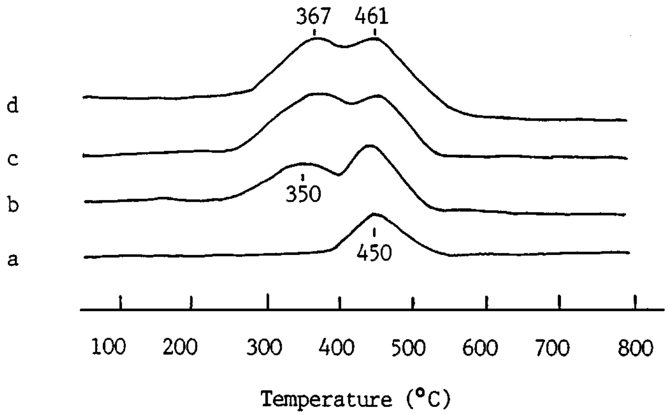

**FIG. 9.** $O_2$ TPD spectra of a 30 mol% $BaCl_2/Y_2O_3$ catalyst used in OCM reaction at 800°C for (a) 0 h, (b) 4 h, (c) 8 h, and (d) 12 h.

## DISCUSSION

For the $Y_2O_3$ catalyst at 800°C, $CH_4$ conversion, $C_2$ selectivity, and $C_2$ yield were 31.8, 26.9, and 8.6%, respectively. Based on the data in Table 1, it is clear that BaO, SrO, and CaO can promote $Y_2O_3$ better than MgO for the OCM reaction. As for the halides of barium, both 30 mol% of $BaCl_2$ and $BaF_2$ can promote $Y_2O_3$ better than 30 mol% of BaO (Table 2). In this paper, we shall concentrate on the effects of $BaCl_2$ on $Y_2O_3$. The effects of $BaF_2$ on $Y_2O_3$ will be reported elsewhere. Over a 30 mol% $BaCl_2/Y_2O_3$ catalyst, $CH_4$ conversion, $C_2$ selectivity, and $C_2$ yield of

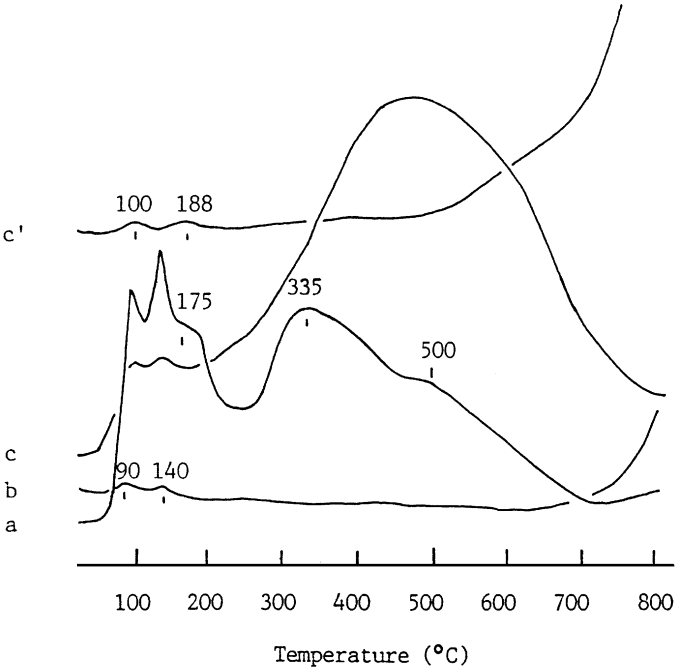

**FIG. 10.** $CO_2$ TPD spectra of (a) $Y_2O_3$, (b) 30 mol% $BaO/Y_2O_3$, and (c) 30 mol% $BaCl_2/Y_2O_3$. Also shown (c′) is the $CO_2$ TPD spectra of a 30 mol% $BaCl_2/Y_2O_3$ catalyst after 8 h in OCM reaction at 800°C.

43.2, 51.7, and 22.3% could be achieved at 800°C. Over a 30 mol% BaO/Y$_2$O$_3$ catalyst, they were 39.1, 31.3, and 12.2%. It seems that BaO can improve both CH$_4$ conversion and C$_2$ selectivity while BaCl$_2$ can further improve the C$_2$ selectivity when the reaction temperatures were above 700°C (Figs. 1 and 2). With the addition of BaCl$_2$ to Y$_2$O$_3$, the specific surface areas of the fresh BaCl$_2$/Y$_2$O$_3$ catalysts reduced. For a fresh 30 mol% BaCl$_2$/Y$_2$O$_3$ catalyst, only cubic Y$_2$O$_3$ crystal phase was detected by XRD. After the OCM reaction, Ba$_3$Cl$_4$CO$_3$ and BaCO$_3$ were detected. For a fresh 30 mol% BaO/Y$_2$O$_3$ catalyst, we detected the BaCO$_3$ crystal phase. Based on the detection of barium compounds and the reduction in specific surface areas of the catalysts when BaCl$_2$ and BaO were added to Y$_2$O$_3$, we can be sure that sintering of surface barium compounds had occurred on Y$_2$O$_3$, especially during OCM reactions. Although chlorine content analysis showed that there was a chlorine loss of up to 13.5% of the original amount after 12 h of reaction, the amount of Cl on the surface, as revealed by XPS studies, was rather constant. This could be the reason why the performance of the catalyst at this point of reaction time was not affected by the loss in chlorine content. The reduction in Ba/Y ratio could be a result of surface sintering of barium compound(s). With the formation of particles, the "surface" of barium compound(s) reduced and so was the Ba3$d_{5/2}$ XPS signal.

Detailed XRD investigations of the BaO/Y$_2$O$_3$ and BaCl$_2$/Y$_2$O$_3$ catalysts revealed that the addition of BaO or BaCl$_2$ to Y$_2$O$_3$ could result in the enlargement of the Y$_2$O$_3$ lattice. Such change in lattice structure of Y$_2$O$_3$ could be a result of ionic substitutions. Ba$^{2+}$ ions (radius, 1.43 Å (41)) are larger than Y$^{3+}$ ions (radius, 0.88 Å (41)) and

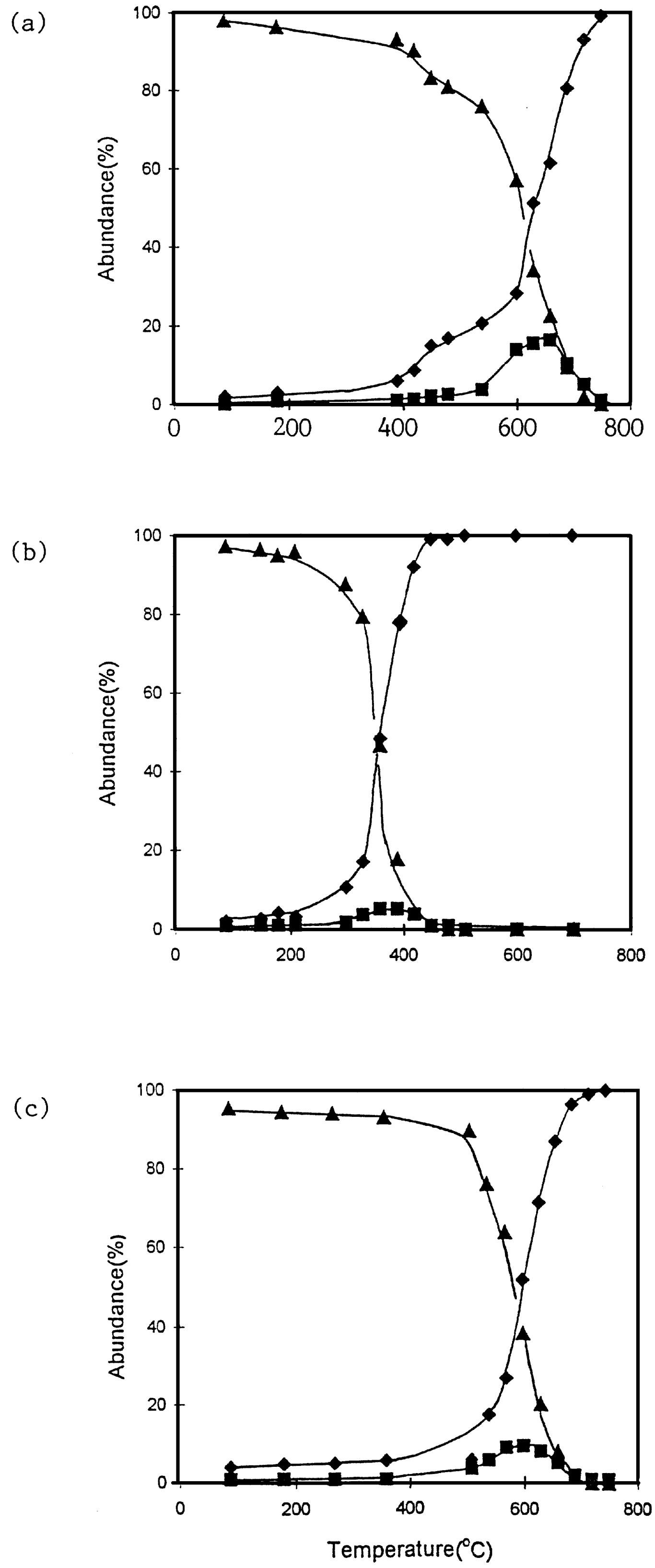

**FIG. 11.** $^{18}$O/$^{16}$O isotope exchange over (a) Y$_2$O$_3$, (b) 30 mol% BaO/Y$_2$O$_3$, (c) 30 mol% BaCl$_2$/Y$_2$O$_3$ catalysts: (◆) $^{16}$O$_2$, (▲) $^{18}$O$_2$, and (■) $^{18}$O$^{16}$O.

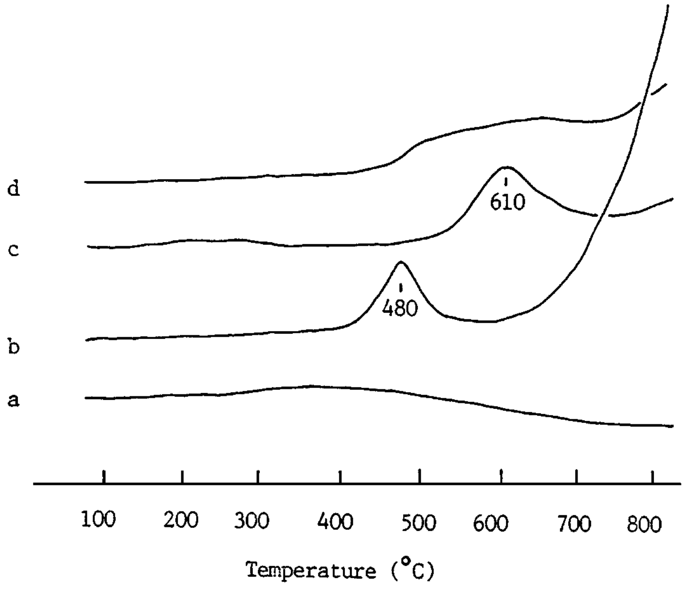

**FIG. 12.** TPR spectra of (a) Y$_2$O$_3$, (b) 30 mol% BaO/Y$_2$O$_3$, (c) 30 mol% BaCl$_2$/Y$_2$O$_3$ catalysts, and (d) a 30 mol% BaCl$_2$/Y$_2$O$_3$ catalyst after OCM reaction at 800°C for 8 h.

carry smaller charge. If certain amount of $Y^{3+}$ ions were replaced by $Ba^{2+}$ ions, being bigger in size and inducing smaller coulombic force, the $Ba^{2+}$ ions occupying lattice points of the $Y_2O_3$ phase will cause the $Y_2O_3$ lattice to expand. We found that $BaCl_2$ addition could enlarge the $Y_2O_3$ lattice even further, especially during the OCM reactions. Hence the reduction in surface Ba/Y ratio detected after the OCM reactions could be partly due to the diffusion of $Ba^{2+}$ ions into the bulk of $Y_2O_3$. Along with the infiltration of the $Ba^{2+}$ ions, certain amount of $O^{2-}$ ions (radius, 1.40 Å (41)) inside the $Y_2O_3$ lattice could be replaced by the incoming $Cl^-$ ions (radius, 1.81 Å (41)). If this happened, an electron would be trapped next to the $Cl^-$ ion to maintain electric neutrality, and the $Y_2O_3$ lattice would enlarge even more. It is clear that such actions of ionic substitution were occurring during the OCM reactions because the $Y_2O_3$ lattices of the 30 mol% $BaO/Y_2O_3$ and 30 mol% $BaCl_2/Y_2O_3$ catalysts were found to enlarge further after the OCM reactions (Fig. 4). Lattice distortions of $Y_2O_3$ have been detected by Osada *et al.* in the $Y_2O_3$–CaO catalysts (26). The increase in $C_{2+}$ selectivity at 600 and 700°C with the addition of $Y_2O_3$ (below 50 mol%) to CaO was attributed to the formation of a solid solution of $Y_2O_3$–CaO and to the presence of interstitial oxygen ions $O_2^-$. In our previous studies, we found that ionic substitutions of similar nature inside the 20 mol% $SrF_2/SmOF$ catalyst would induce the formation of trapped electrons (42). In our studies of a 5 mol% $Y_2O_3/BaF_2$ catalyst, we detected EPR signals of trapped electrons and $O_2^-$ ions (43). Hence, the addition of BaO and $BaCl_2$ to $Y_2O_3$ can alter the surface as well as the bulk natures of $Y_2O_3$. On the surface, barium compounds accumulated and in the bulk, replacements of $Y^{3+}$ by $Ba^{2+}$ ions and $O^{2-}$ by $Cl^-$ ions occurred. As both pure BaO and $BaCl_2$ performed rather poorly below 800°C in OCM reactions (Tables 1 and 2), the accumulation of BaO or $BaCl_2$ on $Y_2O_3$ cannot explain the enhanced performance over the promoted catalysts. In other words, $Y_2O_3$ was not acting solely as support. We advocate the proposal of Kaminsky *et al.* in their $Ba/Y_2O_3$ studies (27) and conclude that the superiority in catalytic performance of the BaO- and $BaCl_2$-promoted $Y_2O_3$ catalyst is due to ionic substitutions occurred inside the lattice of $Y_2O_3$.

It has been pointed out that the reduction in specific surface area of the 0–90 mol% $BaCO_3/LaOCl$ catalysts could improve $C_2$ selectivity but not necessarily reduce $CH_4$ conversion (37). It is because according to the following chemical equations, for a limited amount of oxygen, as more $CH_4$ were converted to $C_2$ compounds due to the suppression in $CH_4$ deep oxidation, $CH_4$ conversion was in fact enhanced:

$$\text{Complete oxidation,}\quad CH_4 + 2O_2 \rightarrow CO_2 + 2H_2O$$

$$C_2\ \text{generation,}\quad 2CH_4 + O_2 \rightarrow C_2H_4 + 2H_2O$$

$$2CH_4 + \tfrac{1}{2}O_2 \rightarrow C_2H_6 + H_2O.$$

The net result was that, although there was reduction in specific surface areas, the conversion of methane changed little. From Fig. 2, between 0 and 40 mol% $BaCl_2$ loadings, the addition of $BaCl_2$ has greatly improved the $C_2$ selectivity and even though there was reduction in specific surface area, the $CH_4$ conversion over the $BaCl_2/Y_2O_3$ catalysts improved. Above 40 mol% $BaCl_2$ loading and at 750°C, both $CH_4$ conversion and $C_2$ selectivity dropped. We believe it is a result of surface accumulation of $Ba_3Cl_4CO_3$ crystals which might not be active in the OCM reaction. As for the $BaO/Y_2O_3$ catalysts, there were steady improvements in $CH_4$ conversion and $C_2$ selectivity as the loading of BaO increased from 0 to 50 mol%. At 750 and 800°C, the 40 and 50 mol% $BaO/Y_2O_3$ catalysts were inferior to the corresponding $BaCl_2/Y_2O_3$ in $C_2$ selectivity but definitely superior in $CH_4$ conversion. The net effect is that at 50 mol% loading, the $BaO/Y_2O_3$ catalyst has higher $C_2$ yield than the $BaCl_2/Y_2O_3$ catalyst.

Based on the $O_2$ TPD results in Fig. 7, we know that considerable amounts of $O_2$ can desorb from the $Y_2O_3$ and 10 to 50 mol% $BaO/Y_2O_3$ catalysts. Compared to these amounts, the $O_2$ desorbed from the 10 to 70 mol% $BaCl_2/Y_2O_3$ catalysts were very small. It is clear that the presence of $Cl^-$ ions has depleted the amount of oxygen species present in the $BaCl_2/Y_2O_3$ catalysts. After prolongedly used in OCM reactions, the 30 mol% $BaCl_2/Y_2O_3$ catalyst changed to somewhat like a 30 mol% $BaO/Y_2O_3$ catalyst (Figs. 9 and 10). Such changes in the nature of the 30 mol% $BaCl_2/Y_2O_3$ catalyst apparently had no drastic effect on the performance of the catalyst (Fig. 5).

Osada *et al.* (26) have reported the formation of $Y_2O_3$–CaO solid solution in their studies of binary oxides $Y_2O_3$–CaO as OCM catalysts. They concluded that the formation of the solid solution would result in a lowering of surface basicity, thereby increasing the activity and selectivity at temperatures below 700°C. In our studies, we found that the 30 mol% $BaO/Y_2O_3$ catalyst performed well at 650°C (Fig. 2), possibly due to similar reasons. From Fig. 10, we know that the $BaO/Y_2O_3$ catalyst has low surface basicity. Based on the $^{18}O/^{16}O$ isotope exchange data over the fresh $Y_2O_3$, 30 mol% $BaO/Y_2O_3$, and 30 mol% $BaCl_2/Y_2O_3$ catalysts, 30 mol% $BaO/Y_2O_3$ appeared to be more likely to get involved in oxidation reaction than the others. This notion is supported by the reduction studies of the three catalysts. Not only the 30 mol% $BaO/Y_2O_3$ catalyst can be reduced at lower temperatures, it also contain more reducible oxygen than the two other catalysts (Table 4). In other words, the 30 mol% $BaO/Y_2O_3$ catalyst is more ready to enhance $CH_4$ conversion and $CH_4$ deep oxidation than the two catalysts. That is why there was considerable decrease in $C_2$ selectivity above 750°C over the BaO-promoted catalyst. The 30 mol% $BaCl_2/Y_2O_3$ catalyst is superior to the 30 mol% $BaO/Y_2O_3$ catalyst in that it can suppress $CH_4$ deep oxidation and enhance $C_2$ selectivity. Such an effect became most apparent at temperatures above 700°C. From 650 to 800°C, there were gradual increases in $CH_4$ conversion (from 19.8 to 43.2%) and $C_2$ selectivity (from 32.1 to 51.7%). As suggested by Kaminsky *et al.* (27), the substitution of $Ba^{2+}$ into $Y^{3+}$ lattice sites in the Ba-doped $Y_2O_3$ catalyst was temperature dependent and could create more active sites at higher temperatures. We interpret that, although more active sites were created for $CH_4$ activation, there was the presence of chloride ions to inhibit deep oxidation reactions. Since $CH_4$ deep oxidation was smothered and the $CH_4$ activated was channeled to $C_2$ formation, there were increases in both $CH_4$ conversion and $C_2$ selectivity.

## CONCLUSION

Based on the catalytic performance of the $MX_2/Y_2O_3$ ($M = $ Mg, Ca, Sr, Ba, and $X = $ F, Cl, Br) catalysts, we have developed the 30 mol% $BaCl_2/Y_2O_3$ catalyst for the OCM reaction. Both BaO and $BaCl_2$ can promote the catalytic performance of $Y_2O_3$ in the OCM reaction. BaO can improve the conversion of $CH_4$ as well as the selectivity to $C_2$ products. The use of $BaCl_2$ can improve the $C_2$ selectivity value even further. It has been found that with the addition of BaO and $BaCl_2$ to $Y_2O_3$, the surface and bulk natures of $Y_2O_3$ changed significantly. Barium compounds were accumulated on the surface and ionic substitution occurred inside the $Y_2O_3$ lattice. We have proven that there was loss (up to ca 15.5% of the original amount) in chlorine from the 30 mol% $BaCl_2/Y_2O_3$ catalyst during 20 h of OCM reaction at 750°C but the performance of the catalyst was stable within the test period of 40 h. Based on the $O_2$ and $CO_2$ TPD studies, we know that the 30 mol% $BaCl_2/Y_2O_3$ catalyst was changing to somewhat like a 30 mol% $BaO/Y_2O_3$ catalyst. From the reduction studies of the catalysts, we found that the 30 mol% $BaO/Y_2O_3$ catalyst has the highest amount of reducible oxygen. The 30 mol% $BaCl_2/Y_2O_3$ catalyst was able to provide a relatively smaller amount of reducible oxygen than the 30 mol% $BaO/Y_2O_3$ one. Hence, the $C_2$ selectivity obtained over the 30 mol% $BaCl_2$-promoted catalyst was high.

## ACKNOWLEDGMENTS

The project was supported by the Hong Kong Baptist University (HKBU) and the Hong Kong Research Grants Council, UGC (HKBU 146/95P). We thank Mr. M. S. Tse for performing the chlorine analysis. Y.W.L. thanks the HKBU for a Ph.D. studentship.

## REFERENCES

1. Aika, K., Moriyama, T., Takasaki, N., and Iwamatsu, E., *J. Chem. Soc., Chem. Commun.*, 1210 (1986).
2. Yingli, B., Kaiji, Z., Yutao, J., Chiwen, T., and Xiangguang, Y., *Appl. Catal.* **39**, 185 (1988).
3. Carreiro, J. A. S. P., and Baerns, M., *J. Catal.* **117**, 258 (1989).
4. Suzuki, T., Wada, T. S., and Watanabe, Y., *Appl. Catal.* **59**, 213 (1990).
5. Korf, S. J., Roos, J. A., Derksen, J. W. H. C., Vreeman, J. A., van Ommen, J. G., and Ross, J. R. H., *Appl. Catal.* **59**, 291 (1990).
6. Zhang, Z. L., Au, C. T., and Tsai, K. R., *Appl. Catal.* **62**, L29 (1990).
7. Maitra, A. M., Campbell, I., and Tyler, R. J., *Appl. Catal. A: General* **85**, 27 (1992).
8. Carreiro, J. A. S. P., Follmer, G., Lehmann, L., and Baerns, M., *in* "Proceedings, 9th International Congress on Catalysis, Calgary 1988" (M. J. Philips and M. Ternan, Eds.), p. 891. Chem. Institute of Canada, Ottawa, 1988.
9. Buyevskaya, O. V., Suleimanov, A. L., Aliev, S. M., and Sokolovskii, V. D., *React. Kinet. Catal. Lett.* **33**, 223 (1987).
10. Sokolovskii, V. D., Buyevskaya, O. V., Aliev, S. M., and Davydov, A. A., *Stud. Surf. Sci. Catal.* **55**, 437 (1990).
11. (a) Otsuka, K., Yokoyama, S., and Morikawa, A., *Chem. Lett.*, 319 (1985). (b) Otsuka, K., Liu, Q., and Morikawa, A., *J. Chem. Soc., Chem. Commun.*, 586 (1986). (c) Otsuka, K., Jinno, K., and Morikawa, A., *J. Catal.* **100**, 353 (1986). (d) Otsuka, K., and Nakajima, T., *J. Chem. Soc. Faraday Trans. 1* **83**, 1315 (1987). (e) Otsuka, K., and Komatsu, T., *Chem. Lett.*, 483 (1987).
12. (a) Lin, C-H., Campbell, K. D., Wang, J.-X., and Lunsford, J. H., *J. Phys. Chem.* **90**, 534 (1986). (b) Campbell, K. D., Zhang, H., and Lunsford, J. H., *J. Phys. Chem.* **92**, 750 (1988). (c) Tong, Y., Rosynek, M. P., and Lunsford, J. H., *J. Phys. Chem.* **93**, 2896 (1989). (d) Tong, Y., Rosynek, M. P., and Lunsford, J. H., *J. Catal.* **126**, 291 (1990). (e) Xu, M., and Lunsford, J. H., *Catal. Lett.* **11**, 295 (1991).
13. (a) Ekstrom, A., and Lapszewicz, J. A., *J. Chem. Soc., Chem. Commun.*, 797 (1988). (b) Ekstrom, A., and Lapszewicz, J. A., *J. Am. Chem. Soc.* **110**, 5226 (1988).
14. (a) Lacombe, S., Geantet, C., and Mirodatos, C., *J. Catal.* **151**, 439 (1994). (b) Lacombe, S., Zanthoff, H., and Mirodatos, C., *J. Catal.* **155**, 106 (1995).
15. Choudhary, V. R., Chaudhari, S. T., Rajput, A. M., and Rane, V. H., *J. Chem. Soc., Chem. Commun.*, 555 (1989).
16. Le Van, T., Che, M., Kermarec, M., Louis, C., and Tatibouet, J. M., *Catal. Lett.* **6**, 395 (1990).
17. Dubois, J. L., and Cameron, C. J., *Chem. Lett.*, 1089 (1991).
18. Deboy, J. M., and Hicks, R. F., *Ind. Eng. Chem. Res.* **27**, 1577 (1988).
19. Deboy, J. M., and Hicks, R. F., *J. Catal* **113**, 517 (1988).
20. Iwamoto, M., Taga, T., and Kagawa, S., *Chem. Lett.*, 1469 (1982).
21. Deboy, J. M., and Hicks, R. F., *J. Chem. Soc., Chem. Commun.*, 982 (1988).
22. Yamashita, H., Machida, Y., and Tomita, A., *Appl. Catal.* **79**, 203 (1991).
23. Machida, K., and Enyo, M., *J. Chem. Soc., Chem. Commun.*, 1639 (1987).
24. Otsuka, K., Komatsu, T., and Shimizu, Y., Successful design of catalysts, *in* "Studies in Surface Science and Catalysis" (T. Inui, Ed.), Vol. 44, p. 43, Elsevier, Amsterdam, 1988.
25. Mimoun, H., Robine, A., Bonnaudet, S., and Cameron, C. J., *Appl. Catal.* **58**, 269 (1990).
26. Osada, Y., Koike, S., Fukushima, T., Ogasawara, S., Shikada, T., and Ikariya, T., *Appl. Catal.* **59**, 59 (1990).
27. Kaminsky, M. P., Zajac, G. W., Campuzano, J. C., Faiz, M., Beaulaige, L., Gofron, K., Jenning, G., Yao, J. M., and Saldin, D. K., *J. Catal.* **136**, 16 (1992).
28. Erarslanoglu, Y., Onal, I., Dogu, T., and Senkan, S., *Appl. Catal. A* **145**, 75 (1996).
29. Fujimoto, K., Hashimoto, S., Asami, K., Omata, K., and Tominaga, H., *Appl. Catal.* **50**, 223 (1989)
30. Burch, R., Squire, G. D., and Tsang, S. C., *Appl. Catal.* **46**, 69 (1989).
31. Burch, R., Chalker, R. S., and Loader, P., New frontiers in catalysis, *in* "Studies in Surface Science and Catalysis" (L. Guczi *et al.*, Eds.), Vol. 75, p. 1079. Elsevier, Amsterdam, 1992.

32. Sugiyama, S., Matsumura, Y., and Moffat, J. B., *J. Catal.* **139**, 338 (1993).
33. Voyatzis, R., and Moffat, J. B., *J. Catal.* **142**, 45 (1993).
34. Au, C. T., Zhang, Y. Q., and Ng, C. F., *Catal. Lett.* **23**, 377 (1994).
35. Au, C. T., He, H., Lai, S. Y., and Ng, C. F., *J. Catal.* **159**, 280 (1996).
36. Au, C. T., He, H., Lai, S. Y., and Ng, C. F., *J. Catal.* **163**, 399 (1996).
37. Au, C. T., He, H., Lai, S. Y., and Ng, C. F., *Appl. Catal.*, accepted.
38. Au, C. T., He, H., Lai, S. Y., and Ng, C. F., *J. Catal.* **167**, 354 (1997).
39. Vogel, A. I., "Vogel's Textbook of Quantitative Inorganic Analysis," 5th ed., Longman, Harlow/New York, 1991.
40. Wells, A. F., "Structural Inorganic Chemistry," 5th ed., Oxford Univ. Press, Oxford, 1984.
41. Cotton, F. A., and Wilkinson, G., "Advanced Inorganic Chemistry," 3rd ed., Interscience, New York, 1972.
42. Au, C. T., and Zhou, X. P., *J. Chem. Soc., Faraday Trans.* **92**, 1793 (1996).
43. Au, C. T., Zhou, X. P., Liu, Y. W., and Ng, C. F., extended abstract submitted to the Asia-Pacific Congress on Catalysis, Nov. 1997, Kyongju, Korea.